ELSEVIER

Physica A 253 (1998) 57–65

PHYSICA A

Nonequilibrium neural network with competing dynamics[1]

P.L. Garrido, J. Marro *, J.J. Torres[2]

Institute "Carlos I" for Theoretical and Computational Physics, Facultad de Ciencias, Universidad de Granada, 18071-Granada, Spain

Received 17 November 1997

Abstract

A stochastic neural-network model with superposition of neuron and synapse kinetics with a priori probabilities p and $1-p$, respectively, is presented. We report on exact and approximate results for $p \to 0$. This includes Hopfield-like models in which synaptic intensities locally fluctuate around Hebbian values. It is illustrated how fluctuations influence the phase diagram and, in particular, that an appropriate choice of details may significantly improve the retrieval process.

PACS: 05.40.+j; 75.10.Nr; 87.10.+e
Keywords: Neural network; Stochastic system; Hopfield model; Synaptic noise

The Hopfield model for associative memory [1] is convenient to evaluate the relevance of *microscopic* details, namely, additions or variations that try to capture some of the essential features of biological systems; cf. [2–7], for instance. Among these details, the consequence of time variation of the neuron couplings are not yet well enough understood. In fact, models either assume that synapse intensities are determined in a previous learning, *plasticity process* that fixes them to constant values thereafter during the neurons evolution, or else two different time scales are invoked for synapses and neurons, respectively, the former being much larger than the latter. However, it is often recognized that such a *quenched* picture is not quite realistic. That is, besides plasticity, biological synapse intensities vary locally on a time scale smaller than that for neuron activity: On one hand, there are local fluctuations of the neurotransmitters concentration which induce substantial changes in the synapses during the time elapsed between the

* Corresponding author.

[1] Supported by the DGICYT, Project No. PB91-0709, and *Junta de Andalucía* of Spain.

[2] Present address: Institute for Nonlinear Science, University of California, San Diego, CA, USA.

PII S0378-4371(98)00036-3

generation of two consecutive action potentials [8]. On the other, biological neurons are typically connected in practice by more that one synapse [9], each having a different nature, either chemical or electrical, which transmit the action potential at different speed. As a net result of these (and other) processes, the mechanisms of emission, release and activation that relate one neuron to the others are fast processes that appear mostly random to the observer [10]. In fact, it has been reported, for example, neuron variability to repeated presentation of the same stimulus [11]. It seems now out of question, however, that such apparent randomness is an essential feature of the system. This is suggested, for instance, by the fact that different kinds of noise might couple each other to produce *stochastic resonance* under certain circumstances [12]. These observations motivated us to study a simple scenario in which the consequences of random synaptic noise – coexisting with the more familiar *thermal* neural noise – could be investigated. We present in this paper a simple stochastic model which, in fact, allows for detailed analysis of the influence of various kinds of time variation of synapses on the performance of a neural-network system, and we describe some main preliminary results from our study.

Consider a binary-neuron configuration, $\mathbf{s} = \{s_{\mathbf{x}} = \pm 1; \mathbf{x} = 1, \ldots, N\}$, that evolves in time competing with synaptic variations in such a way that a conflict results leading, in general, to *nonequilibrium* steady states. More explicitly, some undetermined agents, which include a heat bath at temperature T, induce stochastic time evolution of the probability of state $(\mathbf{s}, \mathbf{J})$ at time t according to the master equation

$$\partial_t P_t(\mathbf{s}, \mathbf{J}) = p \sum_{\mathbf{x}} \left[-\varpi_{\mathbf{J}}(s_{\mathbf{x}} \to -s_{\mathbf{x}}) P_t(\mathbf{s}, \mathbf{J}) + \varpi_{\mathbf{J}}(s_{\mathbf{x}} \to -s_{\mathbf{x}}) P_t(\mathbf{s}^{\mathbf{x}}, \mathbf{J}) \right] + (1-p) \sum_{\mathbf{x},\mathbf{y}} \sum_{J'_{xy}} \left[-\varpi(J_{xy} \to J'_{xy}) P_t(\mathbf{s}, \mathbf{J}) + \varpi(J'_{xy} \to J_{xy}) P_t(\mathbf{s}, \mathbf{J}^{xy}) \right], \tag{1}$$

here $\mathbf{J} = \{J_{xy} \in \Re\,; \mathbf{x},\mathbf{y} = 1, \ldots, N\}$ is the configuration of synapse intensities, and $\mathbf{s}^{\mathbf{x}}(\mathbf{J}^{xy})$ stands for $\mathbf{s}(\mathbf{J})$ after the change $s_{\mathbf{x}} \to -s_{\mathbf{x}}(J_{xy} \to J'_{xy})$. For simplicity, we assume

$$\varpi(J_{xy} \to J'_{xy}) \text{ independent of the current } \mathbf{s}\,, \tag{2}$$

and

$$\varpi_{\mathbf{J}}(s_{\mathbf{x}} \to -s_{\mathbf{x}}) = \Psi(2\beta s_{\mathbf{x}} h_{\mathbf{x}})\,, \qquad \Psi(X) = \Psi(-X)\, e^{-X}, \tag{3}$$

where $\beta = (k_B T)^{-1}$ and $h_{\mathbf{x}} = h_{\mathbf{x}}(\mathbf{s}, \mathbf{J}) = \sum_{\mathbf{y}} J_{xy} s_{\mathbf{y}}$ is a local field; here we only consider in detail the cases $\Psi(X) = e^{-X/2}$ (*rate A*), and $\Psi(X) = \min\{1, e^{-X}\}$ (*rate B*). Conditions (2) and (3) are introduced for simplicity. The first one reducing Eq. (1) to a stochastic *non-generic* case, amounts to assume that synapses undergo very fast variations rather independently of the much more slowly varying neurons, which we believe may sometimes reflect the situation in nature and, in fact, is the case we study below. As a consequence of condition (3), the stationary solution of Eq. (1),

$P_{st}(\mathbf{s})$, is, for $p = 1$ and $J_{xy} = J_{yx}$, the thermodynamic equilibrium state at T for energy $\mathscr{H}_{\mathbf{J}}(\mathbf{s}) = -\frac{1}{2}\sum_{\mathbf{x}} h_{\mathbf{x}} s_{\mathbf{x}}$. This is the familiar Hopfield Hamiltonian if (quenched) intensities J_{xy} are given by a learning rule such as the Hebb's one [13], so that our model has a well-known limiting case.

Our interest is in the limit $p \to 0$ which introduces two relevant time scales in the problem (after the learning process is completed): There is a fine time scale, τ, in which neurons do not appreciably evolve while synapse intensities fluctuate locally; however, neurons evolve (as in the presence of a steady distribution for the synapses) on the coarse scale $t = p\tau$ for $p \to 0$ and $\tau \to \infty$. One may represent such situation (cf. [14] for further details) by means of

$$\partial_t P_t(\mathbf{s}) = \sum_{\mathbf{x}} \left[\overline{\varpi(\mathbf{s}^{\mathbf{x}}; \mathbf{x})} P_t(\mathbf{s}^{\mathbf{x}}) - \overline{\varpi(\mathbf{s}; \mathbf{x})} P_t(\mathbf{s}) \right] \tag{4}$$

with $\overline{\varpi(\mathbf{s}; \mathbf{x})} = \int d\mathbf{J} f(\mathbf{J}) \varpi_{\mathbf{J}}$, where $f(\mathbf{J})$ is the (stationary) distribution for synaptic fluctuations. This allows one investigating the consequences of different choices for $f(\mathbf{J})$. We only consider in the following functions $f(\mathbf{J})$ such that $\overline{J_{xy}} \equiv \int d\mathbf{J} f(\mathbf{J}) J_{xy} = (1/N)\sum_{\mu} \xi^{\mu}_{\mathbf{x}} \xi^{\mu}_{\mathbf{y}}$, where $\boldsymbol{\xi}^{\mu} \equiv \{\xi^{\mu}_{\mathbf{x}} = \pm 1\}$ are $\mu = 1, \ldots, P$ memory patterns, so that fluctuations are around values corresponding to a given learning rule – the Hebbian one in this example – . Two simple cases (to be interpreted below) are

$$f_1(\mathbf{J}) = \prod_{\mathbf{x},\mathbf{y}} \sum_{\mu=1}^{P} a_{\mu} \Delta^{\mu}_{xy} \tag{5}$$

and

$$f_2(\mathbf{J}) = \sum_{\mu=1}^{P} a_{\mu} \prod_{\mathbf{x},\mathbf{y}} \Delta^{\mu}_{xy}\,, \tag{6}$$

where $\Delta^{\mu}_{xy} \equiv \delta(J_{xy} - (1/a_{\mu}N)\xi^{\mu}_{\mathbf{x}}\xi^{\mu}_{\mathbf{y}})$ and $\sum_{\mu} a_{\mu} = 1$.

It turns out sufficient to analyze these two cases to illustrate our main point, namely, that details concerning the synaptic noise affect essentially the system performance, so that appropriate design of these details may significantly improve the retrieval process in neural networks. In order to illustrate this, we have obtained exact results for both symmetric, $J_{xy} = J_{yx}$, and asymmetric couplings for a choice of effective rates $\overline{\varpi}$, and have used the replica trick, mean-field theory, and computer simulations to deal with other cases. Our study shows that evolution of synapses as in Eq. (1) essentially modifies the performance of the Hopfield network, and various nonequilibrium phase transitions [15] arise whose nature strongly depends on $\overline{\varpi}$. In particular, we find that random fluctuations according to f_2 in Eq. (6), which describes fluctuations involving a kind of correlations, may notably reduce the error in retrieval processes, while this is not the case for f_1 in Eq. (5), which lacks such correlations, whose main effect is introducing a tendency to stabilize the Hopfield solutions. It is likely that a similar conclusion, which one expects to hold beyond the Hopfield-model scenario, applies also to the behavior of biological systems. We report in this paper on the most general

results from our study; further technical details and related numerical work are to be reported elsewhere [16].

For *rate A* and f_1, one may show that an *effective Hamiltonian* exists such that $P_{st}(\mathbf{s}) \propto \exp(-\beta \mathscr{H}_{eff})$ [15] with

$$\mathscr{H}_{eff}(\mathbf{s}) = -\frac{1}{2}\sum_{\mathbf{x},\mathbf{y}} \mathscr{J}_{xy} s_{\mathbf{x}} s_{\mathbf{y}} \,, \tag{7}$$

where $2\beta\mathscr{J}_{xy} = \ln(1+\Phi) - \ln(1-\Phi)$, $\Phi = (1/\alpha)\overline{J_{xy}}\tanh\beta\alpha$ and $\alpha \equiv P/N$ for $a_\mu = 1/P$. If the $\xi^\mu_{\mathbf{x}}$s are quasi-orthogonal to each other, it follows that

$$\mathscr{J}_{xy} \approx \mathscr{A}(\alpha)\frac{1}{N}\sum_{\mu} \xi^\mu_{\mathbf{x}}\xi^\mu_{\mathbf{y}}, \qquad \mathscr{A}(\alpha) = \frac{1}{\beta\alpha}\tanh(\beta\alpha)\,. \tag{8}$$

That is, if fluctuations are described by the exceptionally simple distribution (5), the resulting effective intensities are the Hebbian ones, except for the factor $\mathscr{A}(\alpha)$, which is induced by synaptic fluctuations, and one obtains the Hopfield Hamiltonian, but corresponding to (effective) temperature $T_{eff} \equiv T/\mathscr{A}(\alpha)$. Then $\mathscr{A}(\alpha) = 1$, i.e., the Hopfield case, for $\alpha T^{-1} = 0$ that occurs either if synaptic fluctuations are irrelevant compared to thermal noise ($\alpha \neq 0$, $T \to \infty$) or else if the number of stored patterns is small compared with N in the thermodynamic limit ($T \neq 0$, $\alpha \to 0$). Otherwise $\mathscr{A}(\alpha) < 1$, so that fluctuations amount an extra noise added to the thermal one whose variance depends on the degree of correlation between the stored patterns.

The replica trick and the saddle-point method may then straightforwardly be used to obtain the (effective) free energy and relevant order parameters. For example, $m^\nu \equiv N^{-1}\sum_{\mathbf{x}} \xi^\nu_{\mathbf{x}}\langle s_{\mathbf{x}}\rangle = [[\xi^\nu \tanh\beta_{eff}\{z\sqrt{\alpha r} + (\mathbf{m}+\mathbf{h})\cdot\boldsymbol{\xi}\}]]$ is the overlap with a *condensed pattern* ν (such that $m^\nu \neq 0$ in the thermodynamic limit), and other parameters are (using familiar notation) $q = [[\tanh^2\beta_{eff}\{z\sqrt{\alpha r} + (\mathbf{m}+\mathbf{h})\cdot\boldsymbol{\xi}\}]]$, and $r = q(1-\beta_{eff}+\beta_{eff}q)^{-2}$. Here $\mathbf{m} \equiv \{m^\nu; \nu = 1,\ldots,k\}$, and $\mathbf{h} = \{h^\nu; \nu = 1,\ldots,k\}$ are the conjugate fields; $[[\cdots]]$ involves average over the distribution of condensed patterns (as well as an integral corresponding to the Gaussian noise whose origin is the set of non-condensed patterns).

In order to illustrate the implications of the above, consider $h^\nu = 0\,\forall\nu$. For $T = 0$, a spin-glass solution, $m^\nu = 0$ with $q \neq 0$, exists for any $\alpha < \alpha_q = 2.618$; q depends on α, unlike for the Hopfield model (where $q = 1$). That is, the fact that synapses fluctuate tends to impede the spin-glass phase, and the noise is so large when the number of stored memories exceeds about $3N$ that the spin-glass solution does not exist. This fact has a great formal interest, and also a practical one, because the spin-glass phase hampers the efficiency of retrieval processes; the improvement would be real if one could simultaneously extend the pure, Mattis region [17] closer to α_q, which is not the case for this simple version of the model. As expected, the fluctuations vanish as $\alpha \to 0$, and we then recover the Hopfield result. For $T \neq 0$, one has the Hopfield model with T replaced by T_{eff}. The spin-glass phase occurs for $T < T_{sg}(\alpha)$, where $2\alpha T_{sg}^{-1}(\alpha) = \ln(1-\alpha^{3/2}) - \ln(1-2\alpha+\alpha^{3/2})$ for $\alpha \neq 1$, and $T_{sg}^{-1}(\alpha) = \tanh^{-1}\frac{1}{2}$ for

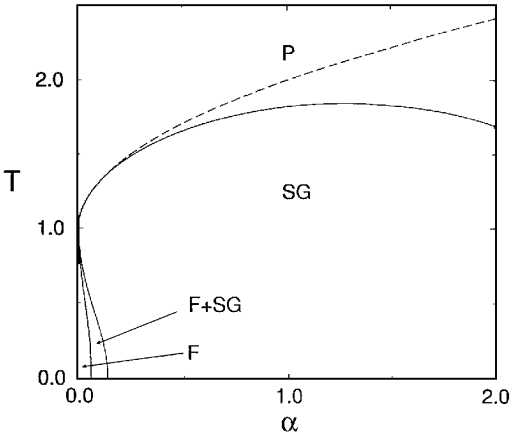

Fig. 1. Phase diagram for *rate A* and f_1 if replica symmetry holds. The solid line, corresponding to the function $T_{sg}(\alpha)$ in the main text, marks continuous phase transitions between the *paramagnetic* phase (P) – which is characterized by zero overlaps with given patterns – , and the *spin-glass* phase (SG) – in which the system retrieves a mixture of stored patterns – . The solid line ends at $T = 0, \alpha = \alpha_q = 2.618$ (not shown), i.e., the spin-glass phase, which is undesired from the point of view of an efficient neural network, does not exist for $\alpha > \alpha_q$; cf. the main text. The dashed line going as $\sim \alpha^{1/2}$ is the corresponding Hopfield result. The lines near the origin depict a discontinuous phase transition such that *ferromagnetic* (F) states – characterized by nonvanishing overlaps – are the only stable ones in the inmost region.

$\alpha = 1$; this transforms into the Hopfield result, $T_{sg}(\alpha) = 1 + \sqrt{\alpha}$, as $\alpha \to 0$. The resulting phase diagram (Fig. 1) is therefore qualitatively similar to the Hopfield one if fluctuations are small enough ($\alpha \to 0$) but differences are significant for large α. Furthermore, the Almeida – Thouless limit of stability of the *ferromagnetic* solution [18] does not occur for any $T \geqslant 0$, because of the excess noise that increases with α. The entropy associated with Mattis states is $T^{-2}(T_{eff}^2 - \alpha^2)$ times the Hopfield result (with T replaced by T_{eff}), so that it goes to zero as $T \to 0$, unlike for the Hopfield case.

The (factorized) function f_1 to which the preceding results concern implies lack of correlation between fluctuations at different synapses: each intensity equals one of the elements in one of the memorized patterns, which results in the mathematical simplicity illustrated above. More interesting a priori are fluctuations that may exhibit correlations, such as f_2 in Eq. (6). Each pattern $\boldsymbol{\xi}^\mu$ then contributes with certain probability to $\mathbf{J}$, which will reflect the spatial correlations within $\boldsymbol{\xi}^\mu$. In the rest of the paper, we illustrate this behavior for $N \to \infty$. (We are strictly concerned with finite P but it seems that our results hold also for the asymptotic regime, $P \to \infty$, as shown below.) From Eq. (4), one obtains

$$\partial_t \langle s_{\mathbf{x}} \rangle = -2\langle s_{\mathbf{x}} a_{\mathbf{x}}^+ \rangle - 2\langle a_{\mathbf{x}}^- \rangle \tag{9}$$

with $2a_{\mathbf{x}}^{\pm}(\mathbf{s}) \equiv \int d\mathbf{J}\, f(\mathbf{J})[\Psi(2\beta s_{\mathbf{x}} h_{\mathbf{x}}) \pm \Psi(-2\beta s_{\mathbf{x}} h_{\mathbf{x}})]$, where $\langle \cdots \rangle$ means average with $P_t(\mathbf{s})$. Consider $N \to \infty$ and the mean-field condition $s_{\mathbf{x}} \approx \langle s_{\mathbf{x}} \rangle$, and develop the steady solution around $\langle s_{\mathbf{x}} \rangle = 0 \forall \mathbf{x}$. This reveals a continuous nonequilibrium phase transition

from paramagnetic- to ferromagnetic-like states at T_c, where $\det\{\overline{J_{xy}}/k_B T_c - \delta_{xy}\} = 0$, and low-$T$ solutions which depend on $\lim_{X\to-\infty}\Psi(X)$. (This limit is $\rho\exp(-\varphi X)$, where $\rho = 1$ and $\varphi = \frac{1}{2}$ for *rate A*, and $\rho = 1$ and $\varphi = 0$ for *rate B*.) For example, $T_c = 1$ when each pattern contributes with the same intensity to every synapse, $a_\mu = 1/P$.

For any set $\{\xi_{\mathbf{x}}^{\mu}\}$ of quasi-orthogonal patterns, one finds under condition $s_{\mathbf{x}} \approx \langle s_{\mathbf{x}}\rangle$ as $N\to\infty$ for finite P, that $\partial_t m^\mu = -2m^\mu\sum_\nu a_\nu \mathscr{B}_\nu^+ - 2a_\mu \mathscr{B}_\mu^-$, where $2\mathscr{B}_\mu^\pm = \Psi(2M^\mu) \pm \Psi(-2M^\mu)$ with $M^\mu \equiv \beta a_\mu^{-1} m^\mu$. This has the stationary solution

$$\mathbf{m} = \left(m^1,\ldots,m^P\right), \qquad m^\mu = \frac{a_\mu \mathscr{B}_\mu^-}{\sum_{\nu=1}^P a_\nu \mathscr{B}_\nu^+}\,. \tag{10}$$

In addition to the trivial solution, one obtains $(m^1,\ldots,m^n,0,\ldots,0)$ with $n\leqslant P$ and $1\geqslant|m^\mu|>0$ for $T<T_c = 1$. Mattis states are for $n = 1$: there are $2P$ such solutions for P stored patterns. Spin-glass or mixture states are for $n > 1$ and $\mathbf{m} = m_n(1,\ldots,1,-1,\ldots,-1,0,\ldots,0)$ for a_μ independent of μ.

More explicit results depend on the choice for Ψ. Consider *rate B*, which transforms Eq. (10) into $|m^\mu| = \Omega_\mu^-/\sum_\nu \Omega_\nu^+$ with $\Omega_\mu^\pm \equiv a_\mu[1\pm\exp(-2|M^\mu|)]$, i.e., m^μ depends on a_μ and on the other $P-1$ overlaps. The low-temperature behavior depends on the type of solution $(m^1,\ldots,m^n,0,\ldots,0)$; for $n = P, |m^\mu| = a_\mu$ at $T = 0$; for $P-n(>0)$ zero overlaps, the other n non-zero overlaps at $T = 0$ are $|m^\mu| = a_\mu/(1+\sum_{\nu=n+1}^P a_\nu)$. For $a_\mu = 1/P, m^\mu$ can only take values 0 and $\pm|m_n|$ for any T, and one has below T_c that

$$|m_n| = \begin{cases} (P-n)^{-1}(1-T), & n<P \\ P^{-1}\sqrt{3(1-T)}, & n=P \end{cases} \quad \text{as } T\to 1^-, \tag{11}$$

which transforms continuously into $|m_n| = (2P-n)^{-1}$, $n\leqslant P$, as $T\to 0$. For *rate A*, $m^\mu = a_\mu \sinh M^\mu(\sum_\nu a_\nu\cosh M_\nu)^{-1}$, so that m^μ depends on a_μ and on the other $P-1$ overlaps, and it follows at zero-T that $m^\mu = a_\mu(\sum_{\nu=1}^{n_\sigma} a_\nu)^{-1}\operatorname{sign}(m^\mu)\delta_{\sigma\mu}$, where σ stands for the pattern such that $|m^\sigma| = \max_\mu|m^\mu|$, and n_σ is the number of overlaps $|m^\mu| = |m^\sigma|$. Therefore, $m^\mu = \operatorname{sign}(m^\mu)\delta_{\sigma\mu}$ for $n_\sigma = 1$, so that the system can then recover a pattern without error at $T = 0$. For $a_\mu = 1/P$ with $m^\mu = 0,\pm|m_n|$, where m_n is a functions of T, n, and P, two different types of mixture may occur for $T > 0$: If $n > \frac{1}{3}P$, $m_n = 0$ for $T>T_c$, and

$$|m_n| = \sqrt{\frac{6(1-T)}{P(3n-P)}} \quad \text{as } T\to 1^-; \tag{12}$$

if $n\leqslant P/3$, however, m_n behaves discontinuously at, say, $\tilde{T}(n,P)$ such that $\tilde{T}(n,P<3n) = T_c$, as in a first-order phase transition. This behavior is illustrated in Fig. 2. Most interesting in this case is the fact that the existence of a discontinuity allows for large overlaps just below $\tilde{T}$. In order to confirm these results obtained after combining (9) with a mean-field type of approximation – which we, however, expected to be realistic for the present highly-connected system – , we performed some exploratory

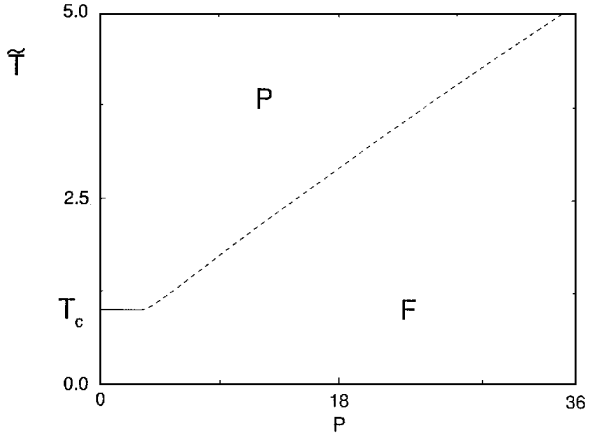

Fig. 2. Phase diagram for $n = 1$ as given by (10), i.e., *rate A* and f_2. The line, corresponding to the function $\tilde{T}(1,P)$ in the main text, indicates (nonequilibrium) phase transitions of second (solid) and first (dashed) order. $\tilde{T}(1,P)$ increases always less than linearly with P; cf. the main text. The existence of a *nonequilibrium tricritical point* is a remarkable feature of our system which causes good retrieval properties for any $P > 3$ at finite temperature.

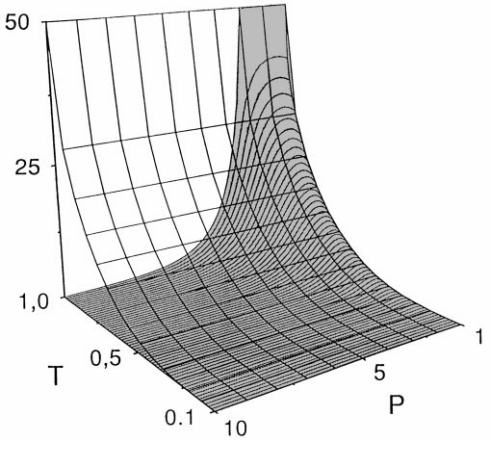

Fig. 3. The percentage of error, as measured by $(1 - m_1)/2$, during retrieval processes for Mattis states for $T < \tilde{T}$ in the case of Fig. 2 (shadow surface), where the error is only large for very small P near T_c, and the corresponding Hopfield result (grid). This comparison illustrates our comment in the caption for Fig. 2.

Monte Carlo simulations concerning a network of 3600 neurons; we thus obtained the same behavior for $m_1(T,P)$ within statistical errors and, in particular, we confirmed the existence of the *nonequilibrium tricritical point* at $P = 3$ for Mattis states which is predicted above. Also remarkable is the result that we report in Fig. 3, which is also fully consistent with our Monte Carlo observations [16].

The solutions (10) correspond, in general, to a saddle point whose details strongly depend on Ψ, so that specific analysis are required. For *rate B*, (local) stability depends

on the sign of the eigenvalues of the matrix of elements $\mathscr{Q}_{ij} = 2a_i \left|M^i\right| \exp(-2\left|M^j\right|) + \delta_{ij}\{2\beta\exp(-2\left|M^j\right|) - \sum_\mu a_\mu[1+\exp(-2\left|M^\mu\right|)]\}$; it follows that only mixture states, $n = P$, are stable. The relevant matrix for *rate A* is $\mathscr{Q}_{ij} = 2(\beta\cosh M^i - \sum_\mu a_\mu \cosh M_\mu)\delta_{ij} - 2a_i M^i \sinh M^j$. For $n = 1$ (Mattis states) this has an eigenvalue changing sign at $T = \tilde{T}(1,P) \equiv m_c P\theta^{-1}$, $P > 3$, where $\theta + (P-1)(\theta\cosh\theta - \sinh\theta) - \sinh\theta\cosh\theta = 0$, and one has from Eq. (10) that $m_c = \sinh\theta(\cosh\theta + P - 1)$. The system exhibits associative memory below $\tilde{T}(1,P)$; cf. Fig. 2. In addition to the fact that locally-stable mixture states do not exist, it is noticeable that good, monotonic behavior is suggested as P is further increased even up to very large values, e.g., $\theta \simeq 2.663 + 1.051\ln P$ fits well for $P \in [10^4, 10^{13}]$. That is, our results seem to hold as $P \to \infty$.

Finally, we mention that some of the above can be extended to the case of asymmetric synapses, namely, when J_{xy} and J_{yx} are independent variables. Consider, for example, $J_{xy} = (1/P)\sum_\mu \eta^\mu_{xy}$ with $\alpha^{-1}\eta^\mu_{xy} = A_1\xi^\mu_{\mathbf{x}}\xi^\mu_{\mathbf{y}} + A_2\xi^\mu_{\mathbf{x}} + A_3\xi^\mu_{\mathbf{y}} + A_4$. For f_1, one obtains after some algebra the expression (7) for $\mathscr{H}_{eff}$ with

$$\beta\mathscr{J}_{xy} = \alpha\beta A_4 + \tfrac{1}{2}\ln\mathscr{K}_{xy}\,, \tag{13}$$

where $\mathscr{K}_{xy} = \sum_{i=1}^4 \lambda^i_+\kappa^i_{xy}(\sum_{j=1}^4 \lambda^j_-\kappa^j_{xy})^{-1}$ with $\kappa^1_{xy} = \sum_\mu \xi^\mu_{\mathbf{x}}\xi^\mu_{\mathbf{y}}, \kappa^2_{xy} = \sum_\mu \xi^\mu_{\mathbf{x}}, \kappa^3_{xy} = \sum_\mu \xi^\mu_{\mathbf{y}}, \kappa^4_{xy} = P$, and $\lambda^1_\pm = \pm\alpha_1 + \alpha_2\alpha_3, \lambda^2_\pm = \pm\alpha_2 + \alpha_1\alpha_3, \lambda^3_\pm = \pm\alpha_3 + \alpha_2\alpha_1, \lambda^4_\pm = 1 \pm \prod_{i=1}^3 \alpha_i$; $\alpha_i \equiv \tanh\alpha\beta A_i$. (Here one would need to work out some requirements in order to have $\mathscr{J}_{xy} = \mathscr{J}_{yx}$, which guaranties that the result is a true effective Hamiltonian.) For f_2, one obtains $P\partial_t m^\mu = -2m^\mu\sum_\nu \mathscr{C}^\nu - 2\mathscr{B}^\mu$ for the overlap with a given pattern, $\boldsymbol{\xi}^\mu$, and $P\partial_t\langle s_{\mathbf{x}}\rangle = -2\langle s_{\mathbf{x}}\rangle\sum_\nu \mathscr{C}^\nu - 2\sum_\nu \mathscr{A}^\nu\mathscr{B}^\nu$ for the mean activity in the net. Here $\mathscr{A}^\mu = (A_3 m^\mu + A_4\langle s_{\mathbf{x}}\rangle)/(A_1 m^\mu + A_2\langle s_{\mathbf{x}}\rangle), 2\mathscr{B}^\mu = \Psi(X^+) - \Psi(-X^-)$, and $2\mathscr{C}^\mu = (1-\mathscr{A}^\mu)\Psi(X^+) + (1+\mathscr{A}^\mu)\Psi(-X^-)$ with $X^\pm \equiv 2\beta P[(A_1 \pm A_3)m^\mu + (A_2 \pm A_4)\langle s_{\mathbf{x}}\rangle]$ for quasi-orthogonal patterns under the mean-field condition $s_{\mathbf{x}} \approx \langle s_{\mathbf{x}}\rangle$. One may obtain further interesting behavior from these equations, e.g., they can, in principle, be solved numerically to obtain m^μ and $\langle s_{\mathbf{x}}\rangle$ as a function of T, P and the asymmetry parameters A_i, which is beyond our objectives in this paper.

Summing up, we have presented a kinetic Hopfield-like network in which the neuron-synapse configuration, (**s**,**J**), varies with time according to the Markov processes (1), with $p(1-p)^{-1}$ the rate of variation of **s** relative to that of **J**. Using different methods, we conclude about the limit $p \to 0$, Eq. (4). This corresponds to fast random fluctuations of synapse intensities according to the distribution $f(\mathbf{J})$. Our study indicates that synaptic time variations competing with neuron activity, which is likely to occur in biological systems, influence importantly the behavior of the network. We have only studied in detail distributions f_1 and f_2, such that intensities fluctuate around a Hebbian learning rule, and two familiar cases of dynamic rules. The simplest case, f_1, admits for one of the rules (A) a simple description in terms of an effective Hamiltonian. For appropriate choice of details, this implies an effective temperature – and a modified phase diagram, Fig. 1 – . When fluctuations accomplish with f_2, which respects the spatial correlations that characterize the memorized patterns, steady states have a nonequilibrium nature, as if acted on by a non-Hamiltonian agent, thus

depending essentially on dynamics. For one of the rules (B), the only stable solution is a mixture that has nonzero overlaps with any of the P stored patterns, i.e., associative memory is not exhibited. For the other rule (A), however, Mattis states exist below a line that has a nonequilibrium tricritical point separating continuous from discontinuous phase transitions (Fig. 2). In the latter case, the overlaps may be large (close to either $+1$ or -1) for large P, and recovering errors remain systematically much smaller than the corresponding ones in the Hopfield case (Fig. 3). We have confirmed the main results from our analytical study by means of Monte Carlo simulations (not presented here). We have also obtained closed equations for asymmetric synapsis. No doubt it would be interesting to study systematically these equations as well as further variations of the basic system (1) by numerical and approximate methods.

References

[1] J.J. Hopfield, Proc. Natl. Acad. Sci. USA 79 (1982) 2554.
[2] D.J. Amit et al., Phys. Rev. A 32 (1985) 1007.
[3] B. Derrida et al., Europhys. Lett. 4 (1987) 167.
[4] H. Gutfreund, M. Mezard, Phys. Rev. Lett. 61 (1988) 235.
[5] F.A. Tamarit, E.M.F. Curado, J. Stat. Phys. 62 (1991) 473.
[6] D. Horn, Physica A 200 (1993) 594.
[7] C.R. Da Silva et al., Int. J. Mod. Phys. C 7 (1996) 43.
[8] P. Peretto, An Introduction to the Modeling of Neural Networks, Cambridge University Press, Cambridge 1992.
[9] C.R. Noback, R.J. Demarest, The Human Nervous System: Basic Principles of Neurobiology, McGraw-Hill, New York 1975.
[10] B. Müller, J. Reinhardt, Neural Networks, An Introduction, Springer, Berlin 1990.
[11] D. Ferster, Science 273 (1996) 1812.
[12] W.L. Ditto, F. Moss, APS News 6 (5)(1997) and references therein.
[13] D.O. Hebb, The Organization of Behavior: A Neurophysiological Theory, Wiley, New York, 1949.
[14] P.L. Garrido, J. Marro, J. Stat. Phys. 74 (1994) 663.
[15] J. Marro, R. Dickman, Nonequilibrium Phase Transitions in Lattice Models, Cambridge University Press, Cambridge, 1998.
[16] J.J. Torres, P.L. Garrido, J. Marro, J. Phys. A 30 (1997) 7801.
[17] D.C. Mattis, Phys. Lett. A 56 (1976) 421.
[18] J.R.L. de Almeida, D.J. Thouless, J. Phys. A 11 (1978) 983.